

ACOUSTIC ANALYSIS OF DISSIPATIVE SILENCERS USING NUMERICAL MODELS OBTAINED BY THE TECHNIQUE OF TRANSFER MATRIX AND THE FINITE ELEMENT METHOD

Nilson Barbieri, e-mail : nilson.barbieri@pucpr.br
Pontifícia Universidade Católica do Paraná – PUCPR
Universidade Tecnológica Federal do Paraná-UTFPR

Renato Barbieri, e-mail : renato.barbieri@pucpr.br
Key Fonseca de Lima, e-mail : key.lima@pucpr.br
Pontifícia Universidade Católica do Paraná - PUCPR

***Abstract.** In this work the acoustic behavior of silencers with absorbent material is analyzed through the transmission loss. The numerical models obtained through transfer matrix technique are validated through the approximation of numerical and experimental data. The numeric results obtained with transfer matrix technique take into account only few propagation modes.*

***Keywords:** Absorbent material; dissipative silencer; transmission loss; Finite Element Method.*

1. INTRODUCTION

In developing a new vehicle design, the exhaust system should fit the space intended for their accommodation. Usually, this space is restricted, since the exhaust system is one of the last components to be considered in the design. Thus, it requires increasingly more compact and efficient models.

A simple dissipative silencer consists of a perforated main duct and an outer chamber filled with absorbing material. Attenuation of acoustic waves in the absorbing material is mainly due to viscous and thermal dissipation. Therefore, the acoustic properties of absorbing material are essential to understand the noise control by dissipative silencers. In general, the complex numbers of characteristic impedance and

wavenumber are employed to account for the dissipation of wave through the absorbing material. Due to the complex structure of absorbing material, these acoustic properties are often determined experimentally (Lee, 2005).

Panigrahi and Munjal (2005) showed three methods to analyse lined ducts with bulk reacting linings for their sound attenuation performance. The methods employed for these studies can be broadly categorized into three major types. In one approach, the duct is assumed to be of infinite length of which a slice of finite length is taken out to get a transfer matrix between the two end points of this slice. In another approach, the one dimensional, coupled wave equations are solved, with the pressure difference between the flow passage and the absorptive lining being supported by a perforated plate. In the third major approach, the three-dimensional wave equation is solved, taking into consideration the finite length boundary effects.

Selamet, Xu and Lee (2004) showed a two-dimensional analytical solution is developed to determine the acoustic performance of a perforated single-pass, concentric cylindrical silencer filled with fibrous material.

Wang, Wu and Wu (2009) established a general approach that can analyze the performance of most of the silencers with/without sound absorbent material.

Panigrahi and Munjal (2007) developed a generalized scheme for analysis of multifarious commercially used mufflers. The one-dimensional (1-D) scheme presented in this paper is based on an algorithm that uses user-friendly visual volume elements along with the theory of transfer matrix based muffler analysis.

Wang and Geng (2008) did comparison and application of the experimental methods for multi-layer prediction of acoustical properties of noise control materials in standing wave-duct systems.

Denia et al. (2007) analyzed the acoustic behavior of perforated dissipative circular mufflers with empty extended inlet/outlet by means of a two-dimensional (2D) axisymmetric analytical approach that matches the acoustic pressure and velocity across the geometrical discontinuities, and the finite element method (FEM).

Kirby (2009) compared the acoustic behavior of automotive dissipative silencers with mean flow using analytic and numerical methods.

This study consists of numerical and experimental analysis of acoustic performance of automotive mufflers with and without the presence of absorbent materials inside the expansion chamber, through computer simulations, using transfer matrix, modal analysis and experimental measurements in laboratory. The procedure to Finite Element Analysis is presented but until the moment the results are not validated.

2. MATHEMATICAL MODEL

Figure 1 shows the schematic of a perforated reactive single-pass straight silencer and Fig. 2 shows the schematic of a perforated dissipative single-pass straight silencer.

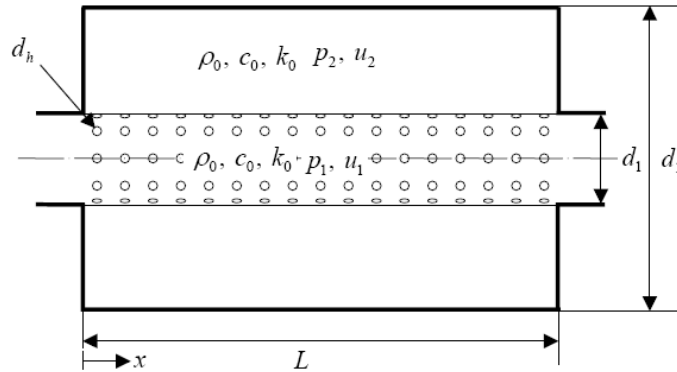


Figure 1 - The schematic of a perforated reactive single-pass straight silencer (Lee, 2005).

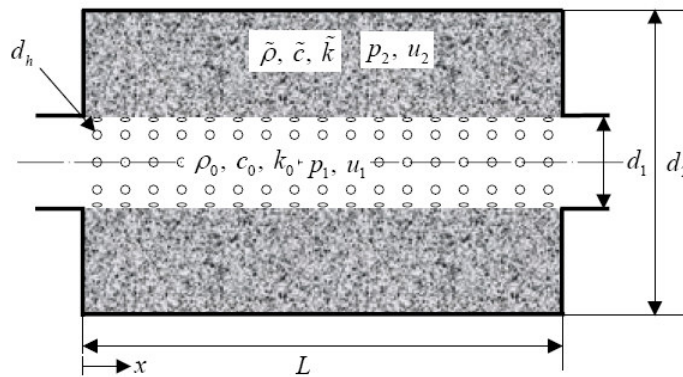


Figure 2 - The schematic of a perforated dissipative single-pass straight silencer (Lee, 2005).

2.1. ONE-DIMENSIONAL ANALYSIS

Assuming harmonic planar wave propagation in both the main duct and the filled outer chamber (Fig. 2), the continuity and momentum equations yield, in the absence of mean flow (Munjal, 1987; Lee, 2005),

$$\frac{d^2 p_1}{dx^2} + \left(k_0^2 - \frac{4ik_0}{d_1 \zeta_p} \right) p_1 + \left(\frac{4ik_0}{d_1 \zeta_p} \right) p_2 = 0; \quad (1)$$

$$\frac{d^2 p_2}{dx^2} + \left(\frac{4d_1}{d_2^2 - d_1^2} \frac{\tilde{\rho}}{\rho_0} \frac{ik_0}{\zeta_p} \right) p_1 + \left(\tilde{k}^2 - \frac{4d_1}{d_2^2 - d_1^2} \frac{\tilde{\rho}}{\rho_0} \frac{ik_0}{\zeta_p} \right) p_2 = 0; \quad (2)$$

where k_0 denote the wavenumber in air; p_1 and p_2 is the acoustic pressure in the main duct (domain 1) and the outer chamber (domain 2), respectively; $\tilde{\zeta}_p = \frac{p_1 - p_2}{\rho_0 c_0 u_1}$ the acoustic impedance of the perforated duct, and u_1 is the particle velocity in the main duct.

Equations (1) and (2) may be rearranged as,

$$\begin{pmatrix} \dot{p}_1 \\ \left(\frac{dp_1}{dx}\right)' \\ \dot{p}_2 \\ \left(\frac{dp_2}{dx}\right)' \end{pmatrix} = \begin{bmatrix} 0 & 1 & 0 & 0 \\ -\left(k_0^2 - \frac{4}{d_1} \frac{ik_0}{\tilde{\zeta}_p}\right) & 0 & -\frac{4}{d_1} \frac{ik_0}{\tilde{\zeta}_p} & 0 \\ 0 & 0 & 0 & 1 \\ -\frac{4d_1}{d_2^2 - d_1^2} \frac{\tilde{\rho}}{\rho_0} \frac{ik_0}{\tilde{\zeta}_p} & 0 & -\tilde{k}^2 - \frac{4d_1}{d_2^2 - d_1^2} \frac{\tilde{\rho}}{\rho_0} \frac{ik_0}{\tilde{\zeta}_p} & 0 \end{bmatrix} \begin{pmatrix} p_1 \\ \frac{dp_1}{dx} \\ p_2 \\ \frac{dp_2}{dx} \end{pmatrix} \quad (3)$$

where ()' indicates derivative with respect to x. Using the linearized momentum equation, Eq. (3) can be rearranged as (Lee, 2005):

$$\begin{pmatrix} \dot{p}_1 \\ \rho_0 c_0 u_1 \\ \dot{p}_2 \\ \tilde{\rho} \tilde{c} u_2 \end{pmatrix} = \begin{bmatrix} 0 & -ik_0 & 0 & 0 \\ -ik_0 - \frac{4}{d_1} \frac{1}{\tilde{\zeta}_p} & 0 & \frac{4}{d_1} \frac{1}{\tilde{\zeta}_p} & 0 \\ 0 & 0 & 0 & -i\tilde{k} \\ \frac{4d_1}{d_2^2 - d_1^2} \frac{\tilde{\rho}}{\rho_0} \frac{k_0}{\tilde{\zeta}_p} & 0 & -i\tilde{k} - \frac{4d_1}{d_2^2 - d_1^2} \frac{\tilde{\rho}}{\rho_0} \frac{k_0}{\tilde{\zeta}_p} & 0 \end{bmatrix} \begin{pmatrix} p_1 \\ \rho_0 c_0 u_1 \\ p_2 \\ \tilde{\rho} \tilde{c} u_2 \end{pmatrix} = [TA] \begin{pmatrix} p_1 \\ \rho_0 c_0 u_1 \\ p_2 \\ \tilde{\rho} \tilde{c} u_2 \end{pmatrix} \quad (4)$$

The solution of Eq. (4) may be expressed in terms of eigenvalues and eigenvectors as

$$\begin{pmatrix} p_1(x) \\ \rho_0 c_0 u_1(x) \\ p_2(x) \\ \tilde{\rho} \tilde{c} u_2(x) \end{pmatrix} = [\Psi] \begin{pmatrix} c_1 e^{\lambda_1 x} \\ c_2 e^{\lambda_2 x} \\ c_3 e^{\lambda_3 x} \\ c_4 e^{\lambda_4 x} \end{pmatrix}; \quad (5)$$

where λ_n is the eigenvalue of the matrix [TA] and [Ψ] the modal matrix whose columns are the eigenvectors. Equation (5) can be rewritten as

$$\begin{pmatrix} p_1(x) \\ \rho_0 c_0 u_1(x) \\ p_2(x) \\ \tilde{\rho} \tilde{c} u_2(x) \end{pmatrix} = [\Psi'(x)] \begin{pmatrix} c_1 \\ c_2 \\ c_3 \\ c_4 \end{pmatrix} \quad (6)$$

which leads to a relationship between the acoustic pressure and the particle velocity at the inlet ($x = 0$) and outlet ($x = L$) as

$$\begin{pmatrix} p_1(0) \\ \rho_0 c_0 u_1(0) \\ p_2(0) \\ \tilde{\rho} \tilde{c} u_2(0) \end{pmatrix} = [TB] \begin{pmatrix} p_1(L) \\ \rho_0 c_0 u_1(L) \\ p_2(L) \\ \tilde{\rho} \tilde{c} u_2(L) \end{pmatrix} \quad (7)$$

$$[TB] = [\Psi'(0)] [\Psi'(L)]^{-1} \quad (8)$$

Finally the transfer matrix of the dissipative silencer is:

$$\begin{pmatrix} p_1(0) \\ \rho_0 c_0 u_1(0) \end{pmatrix} = \begin{bmatrix} T_{11} & T_{12} \\ T_{21} & T_{22} \end{bmatrix} \begin{pmatrix} p_1(L) \\ \rho_0 c_0 u_1(L) \end{pmatrix} \quad (9)$$

2.2. TWO-DIMENSIONAL ANALYSIS

Figure 3 shows the wave propagation in a perforated dissipative silencer in axisymmetric two dimensions.

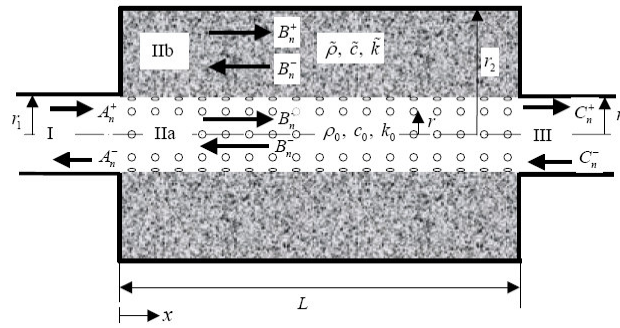


Figure 3 - Wave propagation in a perforated dissipative silencer in axisymmetric two dimensions (Lee, 2005).

For two-dimensional axisymmetric and harmonic wave propagation in a circular, the governing equation duct in the cylindrical coordinates (r, x) can be expressed by (Munjaj, 1987; Lee, 2005):

$$\nabla^2 p(r, x) + k^2 p(r, x) = 0 \quad (10)$$

or

$$\frac{\partial^2 p}{\partial r^2} + \frac{1}{r} \frac{\partial p}{\partial r} + \frac{\partial^2 p}{\partial x^2} + k^2 p = 0 \quad (11)$$

After many manipulations is possible to find the characteristic equation for domain II (Lee, 2005), as:

$$\frac{\rho_0 \sqrt{\tilde{k}^2 - k_{B,x,n}^2}}{\tilde{\rho}} \left[\frac{J_0(\sqrt{k_0^2 - k_{B,x,n}^2} r_1)}{J_1(\sqrt{k_0^2 - k_{B,x,n}^2} r_1)} + i \tilde{z}_p \frac{\sqrt{k_0^2 - k_{B,x,n}^2}}{k_0} \right] = \frac{Y_0(\sqrt{\tilde{k}^2 - k_{B,x,n}^2} r_1) J_1(\sqrt{\tilde{k}^2 - k_{B,x,n}^2} r_2) - Y_1(\sqrt{\tilde{k}^2 - k_{B,x,n}^2} r_2) J_0(\sqrt{\tilde{k}^2 - k_{B,x,n}^2} r_1)}{Y_1(\sqrt{\tilde{k}^2 - k_{B,x,n}^2} r_1) J_1(\sqrt{\tilde{k}^2 - k_{B,x,n}^2} r_2) - Y_1(\sqrt{\tilde{k}^2 - k_{B,x,n}^2} r_2) J_1(\sqrt{\tilde{k}^2 - k_{B,x,n}^2} r_1)} \quad (12)$$

where J_0 and J_1 are the Bessel functions of second kind of orders zero and one, Y_0 and Y_1 are the Bessel functions of first kind of orders zero and one and $k_{B,x,n}$ is the common axial wavenumber.

Lee (2005) proposes to find the TL using a system of equations with several unknown parameters. In this case it is necessary to solve some integrals.

To circumvent the problem of solving integrals, Munjal and Panigrahi and Munjal (2005), introduced a similar system without the need for integration. The relation between the variables of inlet and outlet tube is:

$$\begin{Bmatrix} p_1 \\ v_1 \end{Bmatrix} = [\mathbf{TM}] \begin{Bmatrix} p_4 \\ v_4 \end{Bmatrix} \quad (13)$$

where p_1 and p_4 are the pressures in the inlet and outlet tube and v_1 and v_4 are the velocities, and:

$$[\mathbf{TM}] = \begin{bmatrix} \frac{\alpha_{2-} e^{+jk_{z+} l_p} + \alpha_{2+} e^{-jk_{z-} l_p}}{\alpha_{2-} + \alpha_{2+}} & \frac{e^{+jk_{z+} l_p} - e^{-jk_{z-} l_p}}{S_1(\alpha_{2-} + \alpha_{2+})} \\ \frac{\alpha_{2-} \alpha_{2+} S_1(e^{+jk_{z+} l_p} - e^{-jk_{z-} l_p})}{\alpha_{2-} + \alpha_{2+}} & \frac{\alpha_{2-} e^{+jk_{z+} l_p} + \alpha_{2+} e^{-jk_{z-} l_p}}{\alpha_{2-} + \alpha_{2+}} \end{bmatrix} \quad (14)$$

$$\alpha_{2\pm} = \frac{k_{z\pm} / k_0}{\rho_0 c_0 (1 \mp M(k_{z\pm} / k_0))} \quad (15)$$

where $l_p = L$ is the chamber length; k_{z+} and k_{z-} are equal to $k_{B,x,n}$ is the axial wavenumber in forward or rearward wave moving; M is the Mach number and $S_1 = \pi r_1^2$ is the area of the inlet tube.

2.3. FINITE ELEMENT ANALYSIS (Otsuru and Tomiku, 1999)

The discrete formula of the sound field with sound absorption can be obtained as follows: using the ad joint system which works to describe dissipation, then kinetic, potential, and dissipated energies can be expressed in the following equations:

$$T_e = \frac{1}{4\rho_a \omega^2} \times \iiint_e (\text{grad}p \cdot \text{grad}\bar{p}^* + \text{grad}\bar{p}^* \cdot \text{grad}p) dx dy dz \quad (16)$$

$$V_e = \frac{1}{4\rho_a c_a} \iiint_e (p\bar{p}^* + \bar{p}p^*) dx dy dz \quad (17)$$

$$J_e = \frac{i}{4\rho_a c_a \omega} \iint_e \left(\frac{1}{z_n} p\bar{p}^* - \frac{1}{z_n} \bar{p}p^* \right) dx dy \quad (18)$$

Here, z_n in equation (18) denotes the normal acoustic impedance ratio at the wall's surface. And, the work done by external force can be written in the form of

$$W_e = \frac{1}{4} \iint_e (u_o \bar{p}^* + \bar{u}_o p^* + u_o^* \bar{p} + \bar{u}_o^* p) dx dy \quad (19)$$

Then, the Lagrangian of this system can be

$$L = V - T - W + J \quad (20)$$

According to the ordinary finite elemental procedure, sound pressure at an arbitrary point in an element "e" can be approximated to be

$$p = \{N\} \{p\}_e \quad (21)$$

With this shape function, $\{N\}$, element matrices are defined as follows.

$$[K_a]_e = \iiint_e \begin{bmatrix} \frac{\partial \{N\}^T}{\partial x} & \frac{\partial \{N\}^T}{\partial y} & \frac{\partial \{N\}^T}{\partial z} \end{bmatrix} \begin{bmatrix} \frac{\partial x}{\partial \{N\}} \\ \frac{\partial y}{\partial \{N\}} \\ \frac{\partial z}{\partial \{N\}} \end{bmatrix} dx dy dz \quad (22)$$

$$[M_a]_e = \frac{1}{c_a^2} \iiint_e \{N\}^T \{N\} dx dy dz \quad (23)$$

Assuming the locally reactiveness at the wall's surface, the dissipating matrix can be obtained by

$$[C]_e = \frac{1}{c_a} \iint_e \frac{1}{z_n} \{N\}^T \{N\} dx dy \quad (24)$$

Substituting these matrices into equation (20), and applying Hamilton's principle, the following discrete matrix equation can be derived:

$$[M]\{\ddot{p}\} + [C]\{\dot{p}\} + [K]\{p\} = \rho\omega^2 u\{W\} \quad (25)$$

Or, using velocity potential and velocity of driving force, v , equation (25) can be in the form of

$$[M]\{\ddot{\Phi}\} + [C]\{\dot{\Phi}\} + [K]\{\Phi\} = -v\{W\} \quad (26)$$

In equation (24) the dissipation is modeled using the surface impedance. The other way to denote the dissipation in the system is to use some absorbent finite elements. One that represents a rigid porous material was given by Easwaran and Craggs (1995) using the generalized Rayleigh model;

$$[M_{ab}]_e = \varepsilon K_s \Omega [M_a]_e \quad (27)$$

$$[K_{ab}]_e = \varepsilon [K_a]_e \quad (28)$$

$$[C_{ab}]_e = \varepsilon \frac{R\Omega}{\rho_a} [M_a]_e \quad (29)$$

and

$$\varepsilon = \frac{i\omega\rho_a}{R + i\omega\rho_{ab}} \quad (30)$$

3. RESULTS

The results were obtained for two models of the literature and another obtained in laboratory.

3.1. MUFFLER WITH PERFORATED TUBE WITHOUT ABSORBENT MATERIAL

The model used is shown in Fig.1. The geometric data are: $L = 0.0667\text{m}$, $d_1 = 0.0508\text{m}$, $d_2 = 0.0762\text{m}$; $t_w = 0.00081\text{m}$; $\phi = 0037$; $d_h = 0.00249\text{m}$ (Sullivan and Crocker, 1978). The acoustic impedance of perforations relates the dimensionless acoustic pressure of the inner tube and outer chamber through the interface. The acoustic impedance can be expressed by:

$$\zeta_p = \frac{R + ik_o(t_w + \alpha d_h)}{\phi}$$

where R is the resistance flow; k_o is the wavenumber (air); α is the correction parameter; t_w and d_h are the thicknesses of the perforated wall and the diameter of the holes or perforations, respectively.

Some authors such as Dickey et al. (2001) considers the frequency-dependent resistance. In this work it will be considered constant throughout the frequency range analyzed.

Sullivan and Crocker (1978) presented an empirical expression for the acoustic impedance of the holes (perforations) as:

$$\tilde{\zeta}_p = [0.006 + jk_o(t_w + 0.75d_h)]/\phi$$

In the presence of fiber (for faces with drilling in contact with absorbent material) the equation for acoustic impedance was modified by Selamet et al. (2001) as:

$$\tilde{\zeta}_p = \left[0.006 + jk_o \left\{ t_w + 0.375d_h \left(1 + \frac{\tilde{Z}}{Z_o} \frac{\tilde{k}}{k_o} \right) \right\} \right] / \phi$$

Figure 4 shows the experimental results (Sullivan and Crocker, 1978) and the results obtained numerically using transfer matrix. The numerical results are close to the results presented by Sullivan and Crocker (1978) and Chiu and Chang (2008).

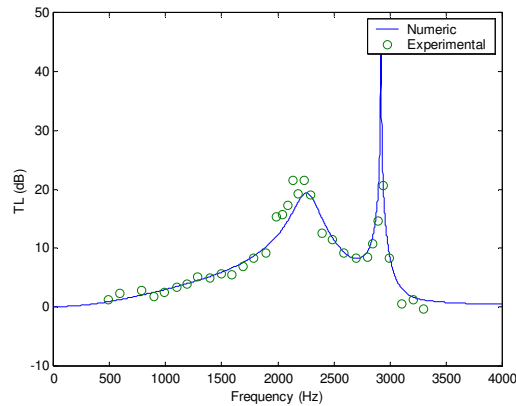


Figure 4 – Transmission loss for a short muffler.

3.2. MUFFLER WITH ABSORBENT MATERIAL

The model used is similar to that shown in Fig. 2. To analyze the behavior of this system we used two examples described in Panigrahi and Munjal (2005). The geometrical dimensions of the first case are: $l = 0.325\text{m}$, $d_1 = 0.0396\text{m}$, $d_2 = 0.0760\text{m}$; $t_w = 0.0009\text{m}$; $\phi = 0.08$, $d_h = 0.00249\text{m}$ (Cummings and Chang, 1988; Panigrahi and Munjal, 2005). The flow resistivity was assumed to be 5000 Pa s/m^2 . The complex wavenumber and characteristic impedance were calculated using the equations set by selamet et. all. (2004):

$$\frac{\tilde{k}}{k} = \left[1 + 0.1472(f/R)^{-0.577} \right] + j \left[-0.1734(f/R)^{-0.595} \right]$$

$$\frac{\tilde{Z}}{Z_0} = \left[1 + 0.0855(f/R)^{-0.754} \right] + j \left[-0.0765(f/R)^{-0.732} \right]$$

where $Z_0 = \rho_0 c_0$ is the characteristic impedance of air and R is the flow resistivity.

The characteristic impedance is given by $\tilde{Z} = \tilde{\rho} \tilde{c}$ the wavenumber is $\tilde{k} = 2\pi f / \tilde{c}$.

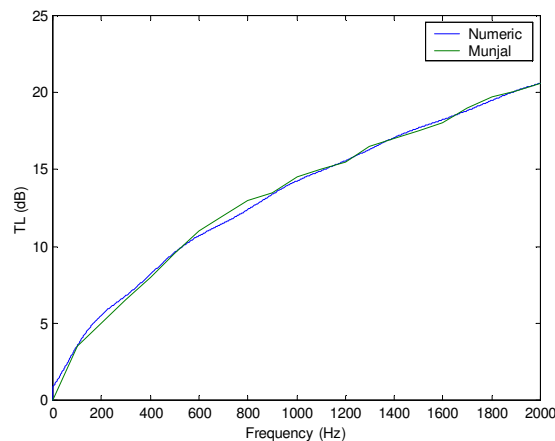


Figure 5 – Transmission loss for a muffler with absorbent material.

Figure 5 shows the curves obtained by Panigrahi and Munjal (2005) and those obtained numerically using the procedure described in equations (13) to (15) and considering the six propagating modes. This case was not considered the drilling of the central tube (without tube). Note that the curves are very close for the entire frequency range analyzed. To find the modes were used two different methods: Newton and Genetic Algorithms. The results were identical. To avoid the jump (jump) between the modes adopted an increment of 1 Hz. Selamet et al. (2004) proposed a method considering the properties of the absorbent null at high frequencies. From a prescribed frequency and using the Newton-Raphson method the eigenvalues are found. The absorbent material properties are incremented until it reached 100% of the values of these constants. Panigrahi and Munjal (2005) use polynomial interpolation and adjusts the values

of the eigenvalues for low frequencies. It was noted that regardless of the procedure adopted the values of the propagating modes always converged to the same values.

The geometric data of the second example are: $L = 0.315\text{m}$, $d_1 = 0.076\text{m}$, $d_2 = 0.1520\text{m}$ (Kirby, 2002; Panigrahi and Munjal, 2005). The flow resistivity of the material is $30\,700\text{ Pa s/m}^2$ and the value of porosity is 26.3% . Again the values of the complex wavenumber and characteristic impedance were calculated using the equations set by Selamet et. al. (2004). Figure 6 shows the experimental curves (Kirby, 2002), numerical (Panigrahi and Munjal, 2005) and numerically with the same procedure described in the previous example. Note that there is a good approximation of the curves. The numeric curve is closer to the experimental data than the curve obtained by Munjal and Panigrahi (2005).

This difference can be attributed to the different expressions used to calculate the complex wavenumber and characteristic impedance.

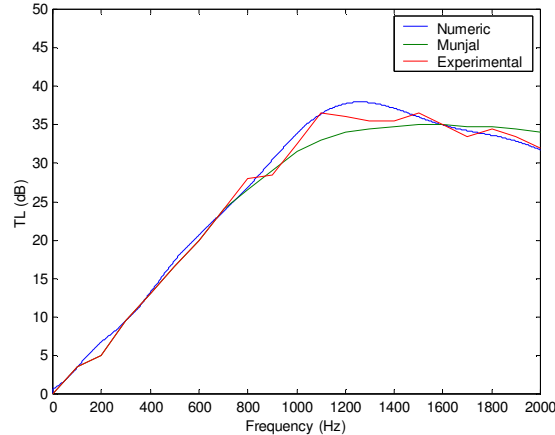


Figure 6 – Transmission loss for a muffler with absorbent material.

3.3. MUFFLER WITH ABSORBENT MATERIAL (MATERIAL CHARACTERIZATION)

To validate the mathematical model was built a prototype with the following dimensions: $l = 0.245\text{m}$, $d_1 = 0.040\text{m}$, $d_2 = 0.189\text{m}$. We used a wire screen to place the absorbent material (glass wool). Thus, there is a need to characterize the material. Using the methodology proposed by Lee (2005) tests were performed on two samples of glass wool (thickness of 3 and 7 cm). The tests were performed with and without an anechoic termination. The sample was positioned near the center of the impedance tube. For this analysis were used four microphones, two before and two after sample.

Figure 7 shows the characteristic impedance and Fig. 8 the complex wavenumber obtained for the sample of 7 cm.

Figure 9 shows the absolute value for the material considering different termination for the two tests: free and with an anechoic termination. A third curve shown represents the average wavenumber found for the system with two terminations. Note that in the range 300 to 2000 Hz the signals are well defined. This frequency range is recommended due to the distance between microphones was 0.06 m .

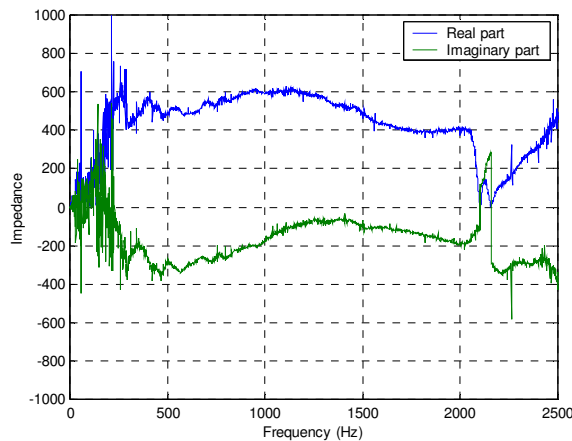


Figure 7 – characteristic impedance.

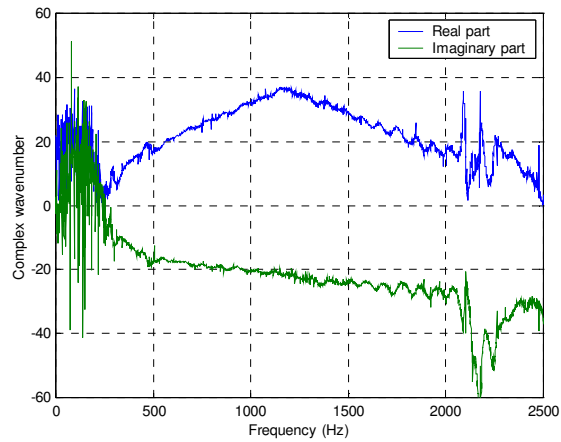


Figure 8 – Complex wavenumber.

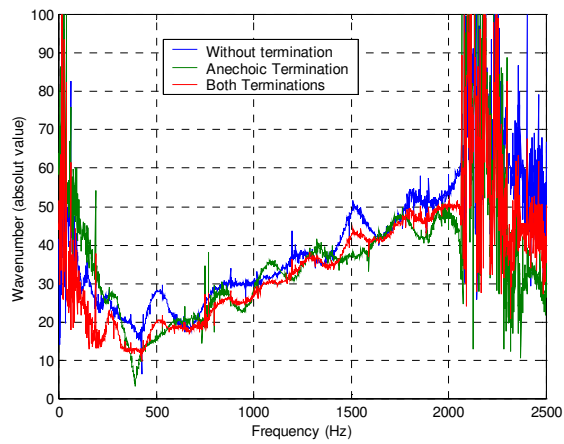


Figure 9 – Wavenumber (three different terminations)

The next step was to find the propagating axial modes(12). It was used a search routine varying the real and imaginary part of the modes of propagation. An error function was defined as the difference between the value of left and right side of equation (12). Figure 10 shows the value of the errors obtained for several iterative steps and increments of the modal parameters. The minimum points correspond to propagating modes.

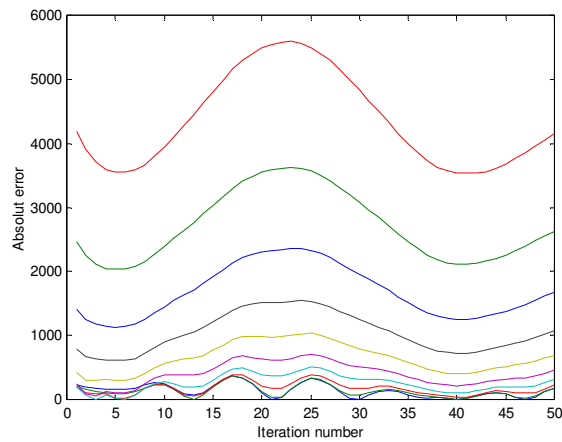


Figure 10 – Error in fitting the propagating modes.

Obtaining the propagation modes for a given frequency, the frequency is varied in increments of 1 Hz to find the modal values for the entire frequency range. Figure 11 shows the first 3 propagation modes.

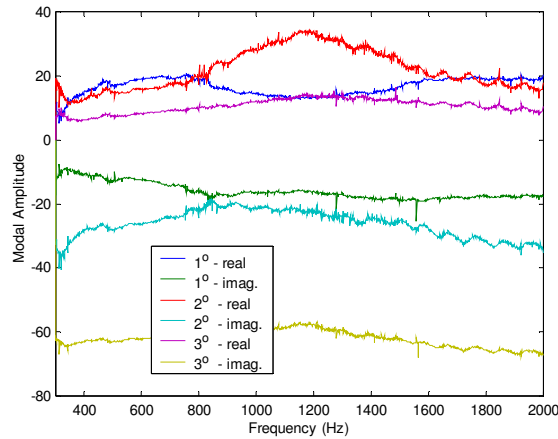


Figure 11 – First three modes.

Using four microphones, two in the inlet and two in the outlet tube, equally spaced, it was calculated the TL using the method of three points. The experimental values of TL for a chamber with absorbent material are shown in Fig. 12.

The numerical values were obtained considering three propagating modes. Souza (2008) showed that for this frequency range the results converge considering only two propagating modes. Note that the experimental and numerical curves have good agreement. The sample material with thickness of 7cm is closer to the real situation.

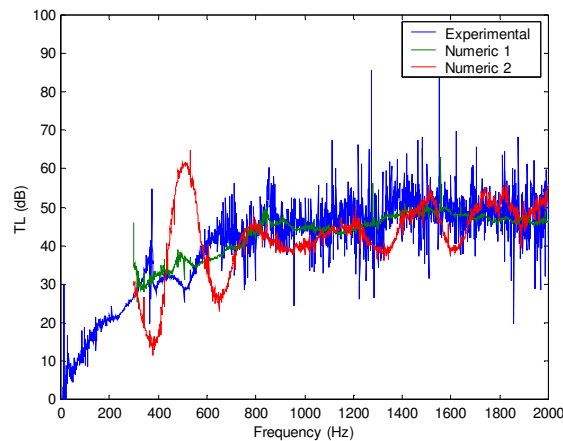


Figure 12 – Transmission loss.

4. CONCLUSIONS

To find the values of transmission loss (TL) it was used analytical methodologies based on modal analysis. The inclusion of absorbent material greatly improves the acoustic behavior of systems, but on the other hand, increases the level of difficulty in mathematical models.

Systems with absorbent material need that analyses are made with more than one propagating mode, although in the system analyzed the responses converged quickly using two or three modes. It was noted that a correct characterization of the material is crucial for calculations of the propagating modes and the TL. The material properties can be modified by increasing or decreasing its compression.

The numerical and experimental results showed good agreement.

5. ACKNOWLEDGEMENTS

The authors gratefully acknowledge the support for this work provided by the Brazilian Science Foundation CNPq.

6. REFERENCES

- Chiu, M.-C. and Chang, Y.-C., 2008, "Numerical studies on venting system with multi-chamber perforated mufflers by GA optimization". *Applied Acoustics*.
- Cummings, A. and Chang, I.J., 1988, "Sound attenuation of a finite length dissipative flow duct silencer with internal mean flow in the absorbent", *Journal of Sound and Vibration*, vol. 127, p. 1–17.
- Denia, F.D., Selamet, A., Fuenmayor, F. J. and Kirby, R., 2007, "Acoustic attenuation performance of perforated dissipative mufflers with empty inlet/outlet extensions". *Journal of Sound and Vibration*, vol. 302, p. 1000-1017.
- Dickey, N. S., Selamet, A. and Ciray, M. S., 2001, "An experimental study of the impedance of perforated plates with grazing flow", *Journal of the Acoustical Society of America*, vol. (110), p. 2360-2370.
- Easwaran, V., Craggs, A., 1995, "On Further Validation and use of the Finite Element Method to Room Acoustics," *J. of Sound and Vib.*, vol. 187(2), p. 195-212.
- Kirby, R., 2009, "A comparison between analytic and numerical methods for modelling automotive dissipative silencers with mean flow". *Journal of Sound and Vibration*, vol. 325, p. 565-582.
- Kirby, R., 2002, "Simplified techniques for predicting the transmission loss of a circular dissipative silencer", *Journal of Sound and Vibration*, vol. 243(3), p. 403–426.
- Lee, I., 2005, "Acoustic characteristics of perforated dissipative and hybrid silencers", Tese de doutorado, The Ohio State University, 195p.
- Otsuru, T., Tomiku, R., 1999, "Modeling and accuracy of sound field analysis by finite element method on building environments". *Building Simulation*, vol. 6, p.p. 1375-1382.
- Panigrahi, S.N. Munjal, M. L., 2007, "A generalized scheme for analysis of multifarious commercially used mufflers". *Applied Acoustics*, vol. 68, p. 660-681.
- Panigrahi, S. N. and Munjal, M. L., 2005, "Comparison of various methods for analyzing lined circular ducts", *Journal of Sound and Vibration*, vol. 285, p. 905–923.
- Selamet, A., Lee, I.J., Ji, Z.L. and Huff, N.T., 2001, "Acoustic attenuation performance of perforated absorbing silencers", *SAE Noise and Vibration Conference*, Paper 2001-01-1435.
- Selamet, A., Xu, M. B., Lee, I.-J. and Huff, N. T., 2004, "Analytical approach for sound attenuation in perforated dissipative silencers", *J. Acoust. Soc. Am.*, vol. 115(5), p. 2091-2099.
- Souza, G. O., 2008, "Análise numérica e experimental de silenciadores automotivos sem e com a presença de materiais de absorção", Dissertação de Mestrado. Pontifícia Universidade Católica do Paraná, 126p.
- Sullivan, J. W. and Crocker, M. J., 1978, "Analysis of concentric-tube resonators having unpartitioned cavities". *J. Acoust. Soc. Am.*, vol. 64(1), p. 207-215
- Wang, C-N, Wu, C-H and Wu, T-D, 2009, "A network approach for analysis of silencers with/without absorbent material". *Applied Acoustics*, vol. 70, p. 208-214.
- Wang, Y. S., He, H. and Geng, A. L., 2008, "Comparison and application of the experimental methods for multi-layer prediction of acoustical properties of noise control materials in standing wave-duct systems". *Applied Acoustics*, vol. 69, p. 847-857.

7. RESPONSIBILITY NOTICE

The authors are the only responsible for the printed material included in this paper.